Heliyon 7 (2021) e08209

Contents lists available at ScienceDirect

Heliyon

journal homepage: www.cell.com/heliyon

Research article

Computational and experimental insight into antituberculosis agent, (*E*)-benzyl-2-(4-hydroxy-2-methoxybenzylidene) hydrazinecarbodithioate: ADME analysis

Tarun Kumar Pal [a,*], Mohammad Abdul Mumit [a], Jewel Hossen [a], Subrata Paul [a], Md. Ashraful Alam [a], Md. Al-Amin-Al-Azadul Islam [a], Md. Chanmiya Sheikh [b]

[a] *Department of Chemistry, Rajshahi University of Engineering & Technology, Rajshahi, 6204, Bangladesh*
[b] *Department of Chemistry, University of Rajshahi, Rajshahi, 6205, Bangladesh*

ARTICLE INFO

Keywords:
(*E*)-benzyl-2-(4-hydroxy-2-methoxybenzylidene)
Hydrazinecarbodithioate
Mass spectra
Antituberculosis

ABSTRACT

A new Schiff base, (*E*)-benzyl-2-(4-hydroxy-2-methoxybenzylidene)hydrazinecarbodithioate (compound **1**) has been synthesized and experimentally characterized by the IR, UV-Vis, ^{1}H-NMR and mass spectroscopies. The theoretical study of the synthesized compound was evaluated using the density functional theory (DFT) at B3LYP/6-31G+(d,p) basis set. The electronic absorption spectrum of compound **1** was evaluated using time-dependent density functional theory. Besides, *in silico* studies were done for the prediction of absorption, distribution, metabolism and excretion profiles of compound **1**. According to the result, the theoretical data were well fitted with the experimental values. The studied compound has low chemical reactivity and high kinetic stability. In the molecular electrostatic potential map, the negative and positive potential sites were found around electronegative atoms and hydrogen atoms of compound **1**, respectively. The 97.75% Lewis and 2.25% non-Lewis structure were present in the studied molecule. The molecular docking results reveal that compound **1** can be used as antituberculosis agent as compare to ethambutol.

1. Introduction

S-benzyl dithiocarbazates (SBDTC) contain hard nitrogen and soft sulfur donor atoms in their backbone. Schiff bases derived from SBDTC can easily bind with transition and non-transition metals [1, 2, 3]. Especially, SBDTC Schiff bases contain four potential donor atoms, two of which are readily available to participate in the formation of metal complexes [2, 4, 5]. SBDTC Schiff bases can form cis-trans and trans-cis isomers due to the N–C and C–S bond and they have significant versatile coordination character and biological activities [6, 7, 8, 9]. An imine group (–RC = N–) containing Schiff bases are also used as dyes, intermediate reactants in the synthesis of organic compounds, catalysts, stabilizing agent in polymeric products, chelating agents in analytical separation methods and inhibitor of corrosion [10, 11]. Moreover, Schiff bases possess noteworthy applications in multifaceted areas such in the solar cell, optical ingredients [6, 7, 9, 12] and medication area such as antiviral, antifungal, antibacterial, insecticidal, anti-HIV, anticancer, antiprotozoal, antimalarial, anti-inflammatory, antidiabetic and antitumor [2, 3, 5, 7, 10, 11, 12, 13, 14, 15]. From the point of view, we report herein the synthesis, characterization as well as investigation of *in silico* quantum calculations of the entitled SBDTC Schiff base in particulars. However, so far we have studied, no theoretical investigation on S-benzyl dithiocarbazate Schiff base has been reported in the literature. Application of DFT is an important quantum mechanical tool for theoretical exploration of various attributes of an organic molecule prior to laboratory experiments. Thus, we report herein DFT investigations involving vibrational, electronic, and ^{1}H-NMR spectra, highest occupied molecular orbital (HOMO) and lowest unoccupied molecular orbital (LUMO) energies, and the chemical descriptors derived from them such as hardness, softness, chemical potential etc., and MEP surface, mulliken population analysis, HOMA index, natural population analysis (NPA) and natural bond orbital (NBO) analysis of the studied compound, (*E*)-benzyl-2-(4-hydroxy-2-methoxybenzylidene)hydrazinecarbodithioate. Moreover, molecular docking analysis was investigated to evaluate the mode of action of the compound at the active site of the target protein as well as ADME prediction was also executed to evaluate the possibility of drug-likeness of the studied compound.

* Corresponding author.
E-mail address: tkpchem@gmail.com (T.K. Pal).

https://doi.org/10.1016/j.heliyon.2021.e08209
Received 19 September 2021; Received in revised form 3 October 2021; Accepted 15 October 2021

2. Experimental

2.1. Materials and methods

Reagent grade chemicals and solvents were procured from Sigma-Aldrich and used without further purification. The IR spectrum of the sample (4000-400 cm^{-1}) was measured by FTIR spectrophotometer (IR Affinity-1S, Shimadzu Corporation, Kyoto, Japan) and UV-Visible absorption (200–1100 nm) was recorded by UV-Visible spectrophotometer (T60, PG Instruments, UK) using 10^{-5} M solution of the sample in dichloromethane in analytical laboratory, Department of Chemistry, Rajshahi University of Engineering & Technology (RUET), Bangladesh. Magnetic susceptibility and molar conductance were determined in magnetic susceptibility balance (Sherwood Scientific, UK) and ECOSCAN CON5 conductivity/temperature meter (Eutech Instruments, Singapore) respectively at room temperature in the same laboratory. ^{1}H-NMR spectrum was determined on a Bruker Ultra-ShieldTM spectrometer (400 MHz) in $CDCl_3$ solvent within the range of (0–13 ppm) with tetramethylsilane (TMS) as internal standard at BCSIR laboratory, Dhaka, Bangladesh. The mass spectrum was obtained on a JEOL-JMS-D300 mass spectrometer from the Department of Applied Chemistry, University of Toyama (Japan).

2.2. Preparation of the Schiff base

An ethanolic solution of potassium hydroxide (1.4 g, 25 mmol) was mixed with 80% solution of hydrazine hydrate (1.25 g, 25 mmol) and cooled to 0 °C in an ice bath. Carbon disulfide solution (1.9 g, 25 mmol) was dropwise added to the mixture with continuous stirring over a 1 h period. The resultant solution was separated into two layers in this time. The lower light-brown layer was collected and dissolved in ethanol (50 ml). Then benzyl chloride (25 g) was added dropwise to the above alcoholic mixture with constant stirring, keeping it in an ice bath. The yellow-colored SBDTC was found. A solution of 4-hydroxy-2-methoxy-benzaldehyde (0.760 g, 5 mmol) was mixed with an ethanolic SBDTC solution (0.99 g, 5 mmol) and subsequently the mixture was refluxed for 6 h with continuous stirring. After refluxing, the mixture was allowed to cool to room temperature for about 2 h. A yellow-color precipitate was separated followed by washing with hot ethanol and allowed to dry under vacuum in presence of anhydrous calcium chloride.

2.3. Computational details

The chemical structure of compound **1** was drawn in GaussView 6.0.16 (Figure 1) and optimized using density functional theory (DFT) with the B3LYP method and 6-31+G(d,p) basis set in Gaussian 09W software tool. Vibrational spectrum, MEP and energies of HOMO and LUMO were explored from the optimized structure of the compound **1**. The electronic excitation of compound **1** was determined applying TD-DFT under the same condition in gas phase. The crystal structure of *Mycobacterium tuberculosis* (PDB ID: 3RUX) was downloaded from the protein data bank website in order to investigate the molecular docking study. The chain A of target protein (3RUX) was selected. This chain was reconstructed by Swiss PDB Viewer 4.10. AutoDock Tools, MG Tools of AutoDock Vina, PyMoL and LigPlot^{+} softwares were utilized in order to investigate the molecular docking ability of the studied compound.

3. Results and discussion

The yield of the synthesized compound was 80%. The melting point of the compound was found to be 158 °C. The studied compound was highly soluble in common organic solvents, such as dichloromethane, chloroform, N,N-dimethylformamide and dimethyl sulfoxide, while it was moderately soluble in water and methanol.

3.1. Infra-red spectrum analysis

The FTIR spectra of compound **1** is depicted in Figure S1. The characteristic band was found at 3138 cm^{-1} (Figure S1, a) due to thione group of the studied compound [12, 16] while the computed value was found to be 3460 cm^{-1} (Figure S1, b). A band at 1618 cm^{-1} in the studied compound is due to aromatic C=C bond [17], theoretically this band was observed at 1625 cm^{-1}. Another characteristic band was observed at 1575 cm^{-1} in the experimental spectrum due to azomethine group [1, 13, 16, 18, 19, 20, 21, 22], theoretically it was found at 1672 cm^{-1}. The symmetric stretching band of ν(C=S) was found to be 1111 cm^{-1} [12,16] in the experimental spectrum while it was found at 1155 cm^{-1} in the computed spectrum. The computed vibrational frequencies are higher than their experimental results, because the computed values are obtained in gas phase while experimental values are obtained in solid phase.

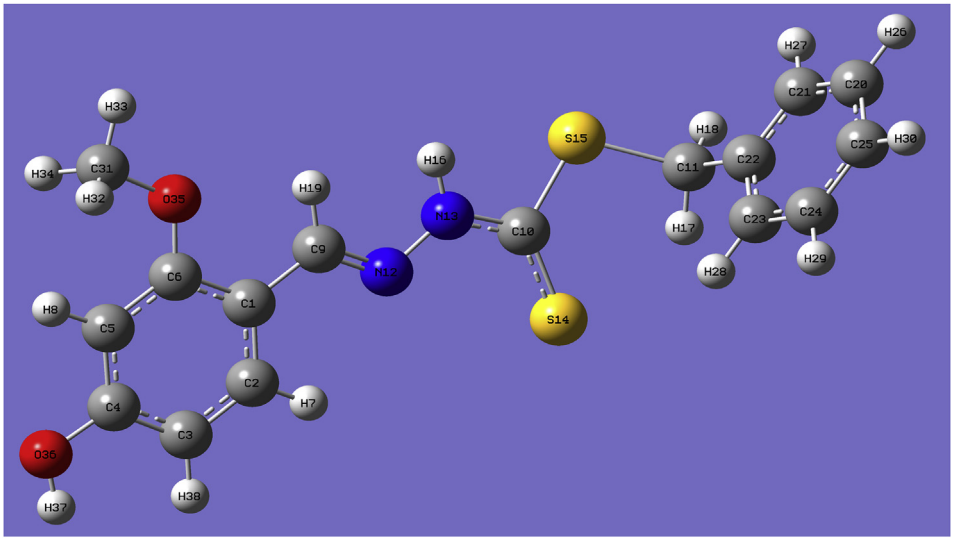

Figure 1. Optimized structure of compound **1**.

3.2. UV-vis spectroscopic study

The spectra of the heading compound are given in Figure S2. The studied compound was shown two peaks in the experimental spectrum at wavelengths of 212 nm and 278 nm (Figure S2, a), which are assigned to π-π* transition originating from the aromatic rings. For this case, the computed value was 315 nm (Figure S2, b),. Compound **1** was shown an absorption band in the spectrum at wavelength of 321 nm, which is assigned to n-π* transition originating from the imine group while this absorption was not observed in the computed spectrum.

3.3. Analysis of ^{1}H-NMR spectrum

The ^{1}H-NMR spectrum of compound **1** showed a singlet at 10.25 ppm due to the –NH(C=S) proton in $CDCl_3$ [23, 24, 25], confirming that the presence of the thione form of compound **1** is present even in solution (Figure S3, a). The calculated chemical shifts for the –NH(C=S) proton was found at 9.26 ppm in $CHCl_3$ (Figure S3, b). The studied compound exhibited a singlet at 8.15 ppm for azomethine (CH = N) proton. The calculated value was 8.63 ppm for CH = N proton. The aromatic protons of SBDTC part observed in the region of 7.25–7.39 ppm. This band was also appeared in the region of 7.65–7.99 ppm in theoretically. The observed singlet signal at 4.48 ppm corresponds to the chemical shift of the S–CH_2 protons, while these protons are calculated at 4.19 ppm in theoretically. The compound **1** showed a singlet at 3.76 ppm due to OCH_3 protons, which was found at 3.97 ppm based on the theoretical spectrum. In addition, the compound exhibited a singlet signal at 6.44, tentatively to the OH proton, which is observed in theoretically at 5.21 ppm. Thus, the ^{1}H-NMR results found by using GIAO method are in good agreement with the experimental values.

3.4. Mass spectrum analysis

The mass spectra inform about the molecular mass, fragmentation pattern as well as the structure of a compound. The mass spectrum of the compound was carried out and the obtained result is presented in Figure S4. The molecular ion peak of the compound, $C_{16}H_{16}N_2O_2S_2$ appeared at 331.1 amu in the mass spectrum. Besides, this compound was shown another characteristic peak at 91.0 amu as base peak. The mentioned compound was also shown various peaks at 301.0, 241.2, 209.1, 148.1 and 123.1 amu corresponding to various fragments as ions or radicals. Both molecular ion and other characteristic peaks of the studied compound were in good agreement with its assigned molecular formula.

3.5. HOMO-LUMO and chemical reactivity indices studies

The energies of HOMO and LUMO can provide important information about the electron donating and accepting capability, biological activity, optical properties (such as luminescence, photochemical reaction etc), quantum chemistry and UV-Visible absorption [23, 24, 25, 26, 27]. In organometallic chemistry addition of pi-bond can be predicted by the LUMO lobe. The energy gap between HOMO and LUMO orbitals is called as a HOMO-LUMO gap which gives information about the stability, chemical reactivity and colors produced by a compound in a solution. The HOMO and LUMO orbitals energy values were found -7.31571 and -4.88077 eV, respectively and the energy gap ($\Delta E_{HOMO\text{-}LUMO}$) was 2.43494 eV. The small energy gap the studied compound represents its high polarizability and chemical reactivity. Distribution of the HOMO and LUMO of the compound was depicted in Figure 2.

The value of chemical hardness, electrophilicity index and chemical potential of studied molecule were calculated and found to be 1.22, 15.27 and -6.10 eV, respectively. The value of chemical softness was 0.41 eV^{-1}. The binding aptitude of a species with different biomolecules determined by the electrophilicity index [22]. The binding capacity of a compound with biomolecules is directly proportional to the electrophilicity index and compound with high electrophilicity index can act as electrophilic species. Moreover, HOMO orbitals partially localized on N12, azomethine group and O–CH_3 group while it has mostly localized on S15, S14 and attached benzene ring. On the other hand, LUMO orbitals were mostly located near the O–CH_3 group attached benzene ring, then S14, azomethine group, S15 and another benzene ring.

3.6. Molecular electrostatic potential investigation

Molecular electrostatic potential (MEP) links with different parameters like electronegativity, partial charges, and dipole moment. It is a pictorial method to interpret the relative polarity of a molecule as well as predictions about the electrophilic and nucleophilic attack. In this study, MEP surface analysis was carried out by the DFT calculation using B3LYP/6-31G+(d,p) which was shown in Figure 3. The red color in the figure indicates electron-rich and blue color indicates electron poor-region. The color code of the studied compound pertains between -1.120e^{-3} to +1.120e^{-3}. The positive surface regions are situated over the H atoms whereas the negative surface areas are visible over the O, S and O–CH_3 group.

3.7. Harmonic oscillator model of aromaticity calculation

Aromaticity is frequently used term in organic chemistry. The harmonic oscillator model of aromaticity (HOMA) can be used to evaluate the aromaticity of homocyclic and heterocyclic organic compounds. HOMA index has been split into GEO and EN destabilizing terms to calculate the geometrical aromaticity of homocyclic molecule. Both terms lead to decrease the HOMA value. Thus, HOMA can be represented as follows:

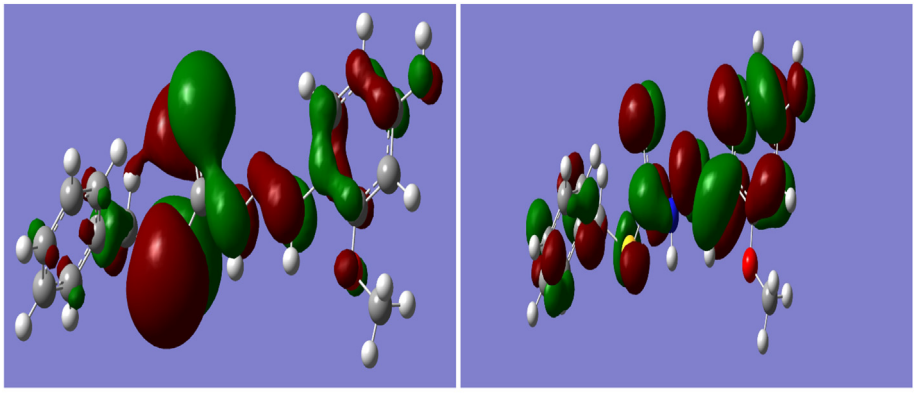

Figure 2. HOMO (a) and LUMO (b) plot of compound **1**.

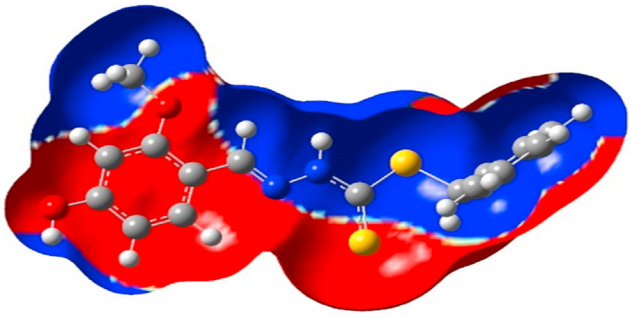

Figure 3. Molecular electrostatic potential surface of compound **1**.

$$\mathrm{HOMA} = 1 - \frac{1}{n}\sum_{i}^{n} \alpha\left(R_{opt} - R_i\right)^2 = 1 - \mathrm{EN} - \mathrm{GEO} \quad (1)$$

where

$$\mathrm{GEO} = \frac{1}{n}\sum_{i}^{n} \alpha\left(R_{av} - R_i\right)^2 \quad (2)$$

and

$$\mathrm{EN} = \alpha\left(R_{opt} - R_{av}\right)^2 \quad (3)$$

The value of HOMA index for pure aromatic compound is close to 1 and that for non-aromatic species is close to 0. The theoretically calculated values of GEO, EN and HOMA of compound **1** were 0.0021, 0.0447 and 0.9343 respectively for C1–C6 ring and 0.0023, 0.0312 and 0.9666 respectively for C20–C25 ring. The experimental and theoretical results conveyed support in favor of aromatic nature for the both rings.

3.8. Natural population and NBO analysis

The natural population analysis (NPA) represents electron distribution in various sub-shells of the atomic orbitals of a molecule. The natural charges on individual atom are presented in Table S1. As per the data, the atom O36 was more electronegative than O35 and the N13 was more electronegative than N12. On the other hand, the C4 and C6 atoms possess around equal alike positive charge. H16 and H37 atoms were also found to be comparatively more electropositive. As per the electrostatic rubric, it's easy to donate electron for electronegative atom and to accept electron for electropositive atom. The accumulations of electrons on the sub-shells of the titled molecule were distributed as follows:

Core: 59.98112 (99.9685% of 60)
Valence: 113.52247 (99.5811% of 114)
Rydberg: 0.49641 (0.2853% of 174)

Natural bond orbital (NBO) analysis extracts valuable information regarding interactions in conjugation and hyper-conjugation, inter- and intra-molecular hydrogen bonding of a compound. In the studied compound, the promotion of LP(2) O35 and O36 to π*C1–C6 and π*C4–C5 were showed 17.98 and 18.07 kcal/mol stabilization energies, respectively (Table S2). These stabilization energies reveal that resonance occurred between aromatic ring and hetero atoms. The electronic transfer from donors to acceptors increases with increasing stabilization energy (E2). Consequently, the entire system of the molecule experiences conjugation to a great extent. The interactions πC1-C6 to π*C2–C3, πC1-C6 to π*C4–C5, πC2-C3 to π*C1–C6, πC2-C3 to π*C4–C5, πC4-C5 to π*C1–C6, and πC4-C5 to π*C2–C3 were found in C1/C6 benzene ring with stabilization energy of 21.99, 16.84; 16.47, 24.33, 23.15, and 15.53 kcal/mol, respectively. In the same way, several transitions were observed in the C20/C25 benzene cycle, such as πC20-C21 to π*C22–C23, πC20-C21 to π*C24–C25, πC22-C23 to π*C20–C21, πC22-C23 to π*C24–C25, πC24-C25 to π*C20–C21 and πC24-C25 to π*C22–C23 containing 20.08, 19.67; 20.37, 19.66, 20.44 and 19.87 kcal/mol energies respectively. These higher stabilization energy interactions of both benzene ring atoms are most responsible for the stability of the title compound. The donor orbital LP(2) S14 demonstrated second strongest interaction with 16.28 kcal/mol stabilization energy, which supports the formation of intra-molecular hydrogen bond between N13–H16 and S14 atom (N13–H16….S14). Besides, the highest stabilization energy containing πC4-C5→π*C2–C3 (269.23 kcal/mol) and πC9-N12→π*C1–C6 (93.03 kcal/mol) interactions lead to intermolecular charge transfer process. The calculated percentage value of hybrid atomic orbitals for the mentioned compound showed that the hybrid atomic orbitals of LP(1) atoms (N12, O35 and O36) were partially contributed to both s and p-type sub-shell (Table S3). Whereas, all anti-bonding orbitals were mainly distributed in p-type sub-shell. The hybrid atomic orbitals of LP(1) S14 and S15 were mainly contributed to the s-sub shell. Basically, p-character of the hybrid orbital of the compound controls the most interacting natural bond orbitals.

3.9. Molecular docking analysis

Nowadays molecular docking has become very popular for drug discovery and drug designing. Molecular docking studies showed good docking scores and interaction of the studied compound with the binding site of the protein of selected pathogenic organisms. The docking of the investigated compound with crystal structure of *Mycobacterium tuberculosis* (PDB ID: 3RUX) was calculated (Figure 4, a). The docking score of compound **1** with the selected protein was –7.5 kcal/mol. The binding mode of compound **1** revealed that the studied compound showed two hydrogen bonds and various hydrophobic interactions with amino acid residues of target protein (Figure 4, b). The Arg69 and Asn130 amino acids of the protein were connected with the ligand via hydrogen bonding within the distance of 3.10 and 2.81 Å. The amino acids of the selected protein, such as Arg72, Ala75, Gly73, Asp167, Val166, Trp74, Ala170, Asn158, Lys138 and Gly68 were joined with the compound via hydrophobic interactions.

While, the drug component, ethambutol was linked with Arg69 amino acid of target protein via two hydrogen bonds within the distance of 2.92 and 3.02 Å (Figure 5, b). Moreover, Asn130 and Lys138 amino acid residues were connected with the drug component through hydrogen bond interactions at 3.12 and 2.89 Å. Additionally, six amino acids, such as Gly68, Gly73, Trp74, Ala170, Asp167, Ala75 were attached with ethambutol. The binding affinity of the ethambutol was found to be -5.3 kcal/mol. Afterward, compound **1** has more binding affinity than the drug component, ethambutol.

3.10. Drug-likeness and ADME analysis

The ability to predict ADME using computer-based software during drug development can greatly reduce both resource and time. The conventional design of drug is time consuming, costly, inconvenient and may take up to 14 years with a cost of 400–650 million USD. A study in Japan showed that a comprehensive non-clinical safety assessment can predict about 48% of adverse drug reactions (ADRs) [28]. Accurate prediction of ADME properties prior to expensive experimental procedures such as HTS (High Throughput Screening) can sort out unnecessary testing on leads that will ultimately fail. Thus, it has become very much necessary to design and synthesize lead compounds which can be easily absorbed, easily distributed or transported to the site of action, give desired pharmacological action, do not metabolize to any toxic metabolites, do not accumulate in the body and excrete easily from the body with least and preferably no major side effects. These above-mentioned properties are collectively termed as ADME. In this study, ADME properties and drug-likeness of Schiff base were calculated using the Qikprop v3.10 tool of Schrödinger. The predicted results are summarized in Table S4. The compound does not violate the Lipinski's rule of five (RO5) and Jorgensen's rule of three. There should be a balance between the solubility and permeability for the optimum absorption of drugs. The compound

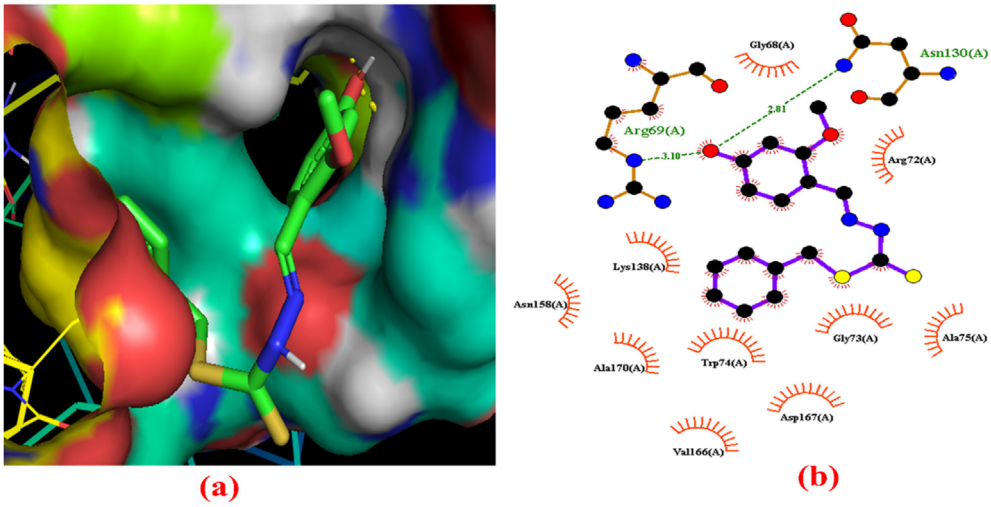

Figure 4. Docking pose (a) and 2D interaction (b) of compound **1** with 3RUX.

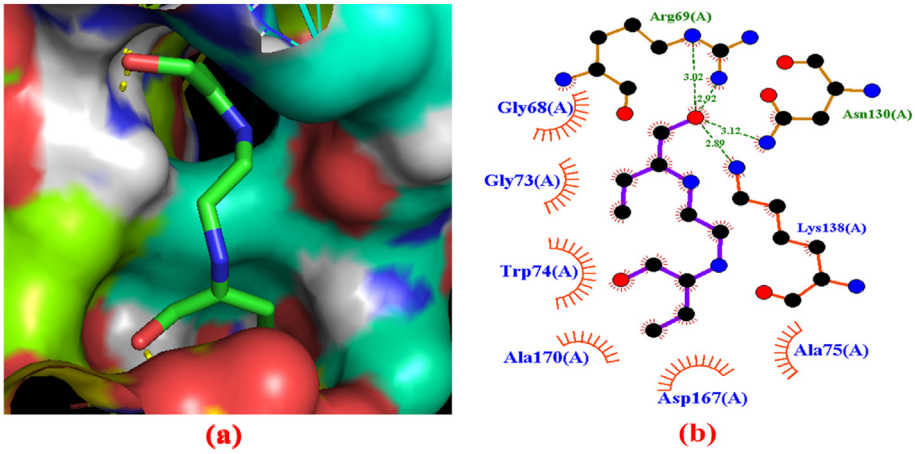

Figure 5. Docking pose (a) and 2D interaction (b) of ethambutol with 3RUX.

showed brilliant solubility, lipophilicity and permeability. So, it is likely to be absorbed well and the predicted value of human oral absorption found 100%. In addition, the compound also possesses good bioavailability due to its favorable number of rotatable bonds and polar surface area. The CNS activity of a drug is predicted on a scale of CNS inactive -2 to CNS active +2. From the predicted value it has been observed that compound **1** doesn't cross the blood-brain barrier and found to be CNS inactive. Other parameters like QPloghERG, QPPCaco, QPPMDCK, and the number of metabolites were also lying within the allowable limit.

4. Conclusion

A new Schiff base, (*E*)-benzyl-2-(4-hydroxy-2-methoxybenzylidene) hydrazinecarbodithioate was characterized by various spectroscopic methods as well as DFT method at B3LYP/6-31G+(d,p) basis set. The azomethine group of the heading compound showed a characteristic band at 1575 cm^{-1} as experimentally while this band was found at 1672 cm^{-1} as theoretically. In the experimental UV-vis spectrum, three peaks were observed at wavelengths of 212 nm, 278 nm and 321 nm, which are assigned to π-π* and n-π* transitions, respectively. The azomethine proton of the studied compound gave a peak 8.15 ppm as experimentally while theoretically it was found at 8.63 ppm. The molecular ion peak of the studied compound was found to be 331.1 amu, which was in good agreement with its assigned molecular formula. The energy difference between HOMO-LUMO (2.43 eV) reveals that the compound has high polarizability and chemical reactivity. The heading compound was also contained 97.75% Lewis and 2.25% non-Lewis character. The molecular docking score of compound **1** with the selected protein (PDB ID: 3RUX) was found to be –7.5 kcal/mol. The molecular docking simulation of the compound **1** showed stronger binding affinity than the standard drug, ethambutol. In addition, the compound **1** showed good ADME profiles and drug-like character.

Declarations

Author contribution statement

Tarun Kumar Pal: Conceived and designed the experiments; Performed the experiments; Analyzed and interpreted the data; Contributed reagents, materials, analysis tools or data; Wrote the paper.

Mohammad Abdul Mumit: Conceived and designed the experiments; Performed the experiments; Contributed reagents, materials, analysis tools or data.

Jewel Hossen: Analyzed and interpreted the data; Contributed reagents, materials, analysis tools or data; Wrote the paper.

Subrata Paul: Analyzed and interpreted the data; Wrote the paper.

Md. Ashraful Alam: Conceived and designed the experiments; Contributed reagents, materials, analysis tools or data.

Md. Al-Amin-Al-Azadul Islam: Conceived and designed the experiments; Performed the experiments; Contributed reagents, materials, analysis tools or data.

Md. Chanmiya Sheikh: Analyzed and interpreted the data; Contributed reagents, materials, analysis tools or data.

Funding statement

This research did not receive any specific grant from funding agencies in the public, commercial, or not-for-profit sectors.

Data availability statement

Data included in article/supplementary material/referenced in article.

Declaration of interests statement

The authors declare no conflict of interest.

Additional information

Supplementary content related to this article has been published online at https://doi.org/10.1016/j.heliyon.2021.e08209.

Acknowledgements

The authors are grateful to the Department of Chemistry, Rajshahi University of Engineering & Technology, Bangladesh for the provision of laboratory facilities, and also thankful to University of Toyama, Japan for providing facilities for NMR and mass analysis.

References

[1] L.H. Abdel-rahman, A.M. Abu-dief, H. Moustafa, A.A.H. Abdel-mawgoud, Design and nonlinear optical properties (NLO) using DFT approach of new Cr (III), VO (II), and Ni (II) chelates incorporating tri-dentate imine ligand for DNA interaction , antimicrobial , anticancer activities and molecular docking studies, Arab. J. Chem. 13 (2020) 649–670.

[2] M. Yazdanbakhsh, R. Takjoo, W. Frank, A.A. Kaju, The preparation, spectroscopic characterization and X-ray crystal structures of the pyrrole-2- carboxaldehyde Schiff base of S-allyldithiocarbazate (HL) and its nickel (II) complex ([Ni(L)2]), J. Coord. Chem. 62 (2009) 3651–3660.

[3] M.S. Begum, E. Zangrando, M.C. Sheikh, R. Miyatake, M.B.H. Howlader, M.N. Rahman, A. Ghosh, Bischelated complexes of a dithiocarbazate N,S Schiff base ligand : synthesis, characterization and antimicrobial activities Bischelated complexes of a dithiocarbazate N,S Schiff base ligand : synthesis, characterization and antimicrobial activities, Transit. Met. Chem. 42 (2017) 553–563.

[4] M.A. Latif, T. Tofaz, B.M. Chaki, H.M.T. Islam, M.S. Hossain, M. Kudrat-E-Zahan, Synthesis, characterization, and biological activity of the Schiff base and its Ni(II), Cu(II) and Zn(II) complexes derived from 4-(dimethylamino) benzaldehyde, Russ. J. Gen. Chem. 89 (2019) 1197–1201.

[5] M.A.F.A. Manan, K.A. Crouse, M.I.M. Tahir, R. Rosli, F.N.-F. How, D.J. Watkin, A.M.Z. Slawin, Synthesis, characterization and cytotoxic activity of S-benzyldithiocarbazate synthesis, characterization and cytotoxic activity of S-benzyldithiocarbazate Schiff bases derived and their crystal structures, J. Chem. Crystallogr. 41 (2011) 1630–1641.

[6] F.N. How, K.A. Crouse, M.I.M. Tahir, M.T.H. Tarafder, A.R. Cowley, Synthesis, characterization and biological studies of S- benzyl- b - N - (benzoyl) dithiocarbazate and its metal complexes, Polyhedron 27 (2008) 3325–3329.

[7] A. Islam, C. Sheikh, M.A. Mumit, R. Miyatake, M.A. Alam, M.O.A. Mondal, Synthesis, characterization and antimicrobial activity of a bidentate NS Schiff base of S-benzyl dithiocarbazate and its divalent complexes, J. Coord. Chem. 69 (2016) 3580–3592.

[8] M. Khaled, M.I.M. Tahir, K.A. Crouse, T. Khoo, Synthesis, characterization , and bioactivity of Schiff bases and their Cd2+, Zn2+, Cu2 , and Ni2+ complexes derived from chloroacetophenone isomers with S-benzyldithiocarbazate and the X-Ray crystal structure of S-Benzyl- ? -N- (4-chlorophenyl)methylened, Bioinorgan. Chem. Appl. 2013 (2013) 1–13.

[9] A.I. Osman, M. Uwaisulqarni, Fatin Zolkipli, Daud Aliyah, Synthesis, characterization and geometry optimization of benzyl 3-[(e,e)-3-phenylprop-2-enylidene]dithiocarbazate (BPED) via DFT studies, J. Sustain. Sci. Manag. 2017 (2017) 80–85.

[10] M. Tahriri, M. Yousefi, K. Mehrani, M. Tabatabaee, M.D. Ashkezari, Synthesis, characterization and antimicrobial activity of two novel sulfonamide schiff base compounds, Pharm. Chem. J. 51 (2017) 425–428.

[11] R. Al-Masoudi, R.H.A.A. Wasfi Aboud, H.S.J. Adnan Faaz, Synthessis, antimicrobial activity and modelling studies of some new metal complexes of Schiff base derived from sulphonamide drug in vitro, Eur. J. Chem. 7 (2016) 102–106.

[12] M.H. Islam, M.C. Sheikh, M.A.A.A.A. Islam, Studies on coordination chemistry and antibacterial activity of bidentate NS Schiff base derived from SBDTC and 4-benzyloxybenzaldehyde, J. Sci. Res. 11 (2019) 121–132.

[13] H.F. Adly, M.I. Omima, El-shafiy, New metal complexes derived from S-benzyldithiocarbazate (SBDTC) and chromone-3- carboxaldehyde: synthesis, characterization, antimicrobial, antitumor activity and DFT calculations, J. Coord. Chem. 72 (2019) 218–238.

[14] A.T. Bader, B.I. Al-abdaly, I. Jassim, Synthesis and characterization new metal complexes of heterocyclic units and study antibacterial and antifungal, J. Pharmaceut. Sci. Res. 11 (2019) 2062–2073.

[15] N. Kausar, S. Muratza, M.A. Raza, H. Rafique, M.N. Arshad, A.A. Altaf, A.M. Asiri, S.S. Shafqat, S.R. Shafqat, Sulfonamide hybrid schiff bases of anthranilic acid: synthesis, characterization and their biological potential, J. Mol. Struct. 1185 (2019) 8–20.

[16] R. Singh, Synthesis , spectral studies and quantum-chemical investigations on S-benzyl b -N- (4-NN biscynodi ethylaminophenylmethylene) dithiocarbazate, Arab. J. Chem. 12 (2019) 1537–1544.

[17] N. Özdemir, R. Kaıit, O. Dayan, Investigation of enol-imine/keto-amine tautomerism in (E)-4-[(2-hydroxybenzylidene)amino]phenyl benzenesulphonate by experimental and molecular modelling methods, Mol. Phys. 114 (2016) 757–768.

[18] F. Cuenú, J. Londoño-salazar, J.E. Torres, R. Abonia, R.F.D. Vries, Synthesis, structural characterization and theoretical studies of a new Schiff base 4- (((3-(tert-Butyl)-(1-phenyl)pyrazol-5-yl) imino)methyl)phenol, J. Mol. Struct. 1152 (2018) 163–176.

[19] I. Rama, R. Selvameena, Synthesis , structure analysis , anti-bacterial and in vitro anti-cancer activity of new Schiff base and its copper complex derived from sulfamethoxazole, J. Chem. Sci. 127 (2015) 671–678.

[20] M. Mesbah, T. Douadi, F. Sahli, S. Boukazoula, Synthesis , characterization , spectroscopic studies and antimicrobial activity of three new Schiff bases derived from Heterocyclic moiety, J. Mol. Struct. 1151 (2018) 41–48.

[21] C. Ali, Ru(III), Cr(III), Fe(III) complexes of Schiff base ligands bearing phenoxy Groups : application as catalysts in the synthesis of vitamin K3, J. Saudi Chem. Soc. 22 (2018) 757–766.

[22] S. Alyar, S. Tülin, Synthesis , spectroscopic characterizations , enzyme inhibition , molecular docking study and DFT calculations of new Schiff bases of sulfa drugs, J. Mol. Struct. 1185 (2019) 416–424.

[23] H. Ebrahimi, J.S. Hadi, A new series of Schiff bases derived from sulfa drugs and indole-3-carboxaldehyde: synthesis, characterization, Spectr. DFT Comput. Stud. 1039 (2013) 37–45.

[24] S.A. Beyramabadi, M. Javan-Khoshkholgh, N.J. Ostad, A. Gharib, M. Ramezanzadeh, M. Sadeghi, A. Bazian, A. Morsali, Spectroscopic (Ft-Ir, Nmr, Uv-vis, Fluorescence) and Dft studies (molecular structure, Ir and Nmr spectral assignments, Nbo and Fukui function) of schiff bases derived from 2-Chloro-3-Quinolinecarboxaldehyde, J. Struct. Chem. 59 (2018) 1342–1352.

[25] H.P. Ebrahimi, J.S. Hadi, A.A. Almayah, Z. Bolandnazar, A.G. Swadi, A. Ebrahimi, Metal-based biologically active azoles and β-lactams derived from sulfa drugs, Bioorg. Med. Chem. 24 (2016) 1121–1131.

[26] Z. Demircioļlu, Ç.A. Kaştaş, O. Büyükgüngör, The spectroscopic (FT-IR, UV-vis), Fukui function, NLO, NBO, NPA and tautomerism effect analysis of (E)-2-[(2-hydroxy-6-methoxybenzylidene)amino]benzonitrile, Spectrochim. Acta Mol. Biomol. Spectrosc. 139 (2015) 539–548.

[27] S. Kumar, V. Saini, I.K. Maurya, J. Sindhu, M. Kumari, R. Kataria, V. Kumar, Design , synthesis , DFT , docking studies and ADME prediction of some new coumarinyl linked pyrazolylthiazoles : potential standalone or adjuvant antimicrobial agents, PLoS One 13 (2018) 1–23.

[28] C. Tamaki, T. Nagayama, M. Hashiba, M. Fujiyoshi, M. Hizue, H. Kodaira, M. Nishida, K. Suzuki, Y. Takashima, Y. Ogino, D. Yasugi, Y. Yoneta, S. Hisada, T. Ohkura, K. Nakamura, Potentials and limitations of nonclinical safety assessment for predicting clinical adverse drug reactions: correlation analysis of 142 approved drugs in Japan, J. Toxicol. Sci. 38 (2013) 581–598.